RSC Advances

PAPER

View Article Online
View Journal | View Issue

Cite this: *RSC Adv.*, 2022, **12**, 11715

Synthesis of ultrahigh-molecular-weight ethylene/1-octene copolymers with salalen titanium(IV) complexes activated by methyaluminoxane†

Baokang Zou,[a] Yipeng Zhan,[a] Xiuli Xie,[a] TongTong Zhang,[a] Runkai Qiu[a] and Fangming Zhu *[ab]

Two salalen titanium(IV) complexes ((H-salalen)$TiCl_2$ and (F-salalen)$TiCl_2$) containing hydrogen and fluorine respectively on the phenolate ring close to the imine were synthesized for the copolymerization of ethylene with 1-octene to prepare poly(ethylene-*co*-1-octene) in the presence of methylaluminoxane (MAO). The (F-salalen)$TiCl_2$/MAO showed higher catalytic activity and better copolymer characteristics such as a higher molecular weight, narrower molecular weight distribution, and higher 1-octene incorporation than (H-salalen)$TiCl_2$/MAO, which revealed that the electron-withdrawing conjugated effect introduced by fluorine substituents led to improvements on catalytic performance and thermal stability. The influences of copolymerization conditions including temperature, Al/Ti molar ratios and comonomer feed ratios on the copolymerization behavior of (F-salalen)$TiCl_2$/MAO and the copolymer microstructure were investigated in detail. Under the activation of MAO, the (F-salalen)$TiCl_2$ could produce ultrahigh molecular weight poly(ethylene-*co*-1-octene) with 1-octene incorporation ratios in the range of 0.9–3.1 mol% and exhibit relatively high activity. It could be inferred that long ethylene sequences in the copolymer were segregated by the isolated 1-octene units based on the ^{13}C NMR characterization of the copolymer. Moreover, the thermal properties and crystallization of copolymers were determined by DSC and XRD and correlated to the ethylene sequence length distribution. The reactivity ratios calculated by the triad distribution in ^{13}C NMR revealed the random comonomer distribution in the copolymer chain.

Received 10th January 2022
Accepted 5th April 2022

DOI: 10.1039/d2ra00165a

rsc.li/rsc-advances

Introduction

Polyethylene including high-density polyethylene (HDPE), linear low-density polyethylene (LLDPE), and low density polyethylene (LDPE) is the most widely used polymer material in the world owing to its excellent comprehensive performance and wide application fields, and its global annual production has exceeded 100 million tons.[1] Furthermore, ultrahigh-molecular-weight polyethylene (UHMWPE) with a well-defined linear structure and ultrahigh-weight-average molecular weight (M_w) more than 1.0×10^6 g mol^{-1} has attracted great attention because of its exceptional wear resistance, impact resistance, chemical stability and lubricity as well as successful application in engineering plastics.[2–4] However, the UHMWPE is difficult to process as a result of high chain entanglement density giving rise to poor melt fluidity.[5] It is worth noting that the processing performance of UHMWPE can be significantly improved *via* the introduction of a small amount of long chain branches. Nevertheless, the introduction of long chain branches (carbon atoms ≥ 6) into the UHMWPE molecular chain is difficult to achieve by copolymerization of ethylene with higher α-olefins such as 1-octene and 1-decene.[6–8] Therefore, in the past few decades, many catalyst systems with high activity and controllable comonomer incorporation rate have been continuously developed for the copolymerization of ethylene with α-olefin, trying to obtain ultrahigh-molecular-weight polyethylene with improved processing properties.

Ziegler–Natta catalysts especially supported Ziegler–Natta catalysts displayed high activity when promoting copolymerization of ethylene with short chain α-olefins. However, copolymers obtained by heterogeneous multi-center Ziegler–Natta systems typically have low commoner content, non-uniform commoner distribution and broad molecular weight distribution, which greatly affects copolymer properties.[9,10] Thus single site catalysts include metallocene catalysts and post metallocene catalysts are preferred to produce ethylene/α-olefin copolymers with better mechanical and rheological properties.[11–18] In 1992, the Dow Chemical Company (Dow) launched a constrained geometry catalyst (CGC) system viable in commercial operations.[19] In contrast with the former metallocene catalyst, Dow's CGC linked mono-cyclopentadienyl

[a]*PCFM, GDHPPC Lab, School of Chemistry, Sun Yat-Sen University, 510275, China. E-mail: ceszfm@mail.sysu.edu.cn; Fax: +86-20-84114033; Tel: +86-20-84113250*
[b]*Key Lab for Polymer Composite and Functional Materials of Ministry of Education, School of Chemistry, Sun Yat-Sen University, Guangzhou, 510275, China*

† Electronic supplementary information (ESI) available. See https://doi.org/10.1039/d2ra00165a

group by a bridge to the amide, which gives the catalyst larger coordination space. This structure is beneficial to produce ethylene/1-octene copolymer with controlled 1-octene incorporation and relatively narrow molecular weight distribution to afford polyolefin elastomer (1-octene content from 20 to 30 wt%) and plastomer polyolefin (1-octene content lower than 20 wt%). However, the copolymer obtained by CGC also has a lower molecular weight, which limits the application range of the material to some extent.[20] Since then many new CGC and post metallocene catalysts have been designed and developed, especially many group IV transition metal complexes bearing O,*N*-chelating or *N*,*N*-chelating ligands exhibited surprisingly excellent catalytic performance on the copolymerization of ethylene with α-olefin, and made significant improvement on the polymer molecular weight and comonomer content.[8,21–25]

The salalens are tetradentate [ONN′O]-type ligands can be regard as half-salan/half-salen, raping the metal center in a *fac–mer* mode with perfect octahedral structure.[26,27] Salalen type complexes exhibit amazing catalytic performance on various reactions like ring-opening polymerization, asymmetric oxidations, epoxide-CO_2 polymerization and α-olefin homopolymerization.[28–39] But to the best of our knowledge, there are few literature has been reported using salalen type complexes on the copolymerization of ethylene with long chain α-olefin. Our research group previously synthesized two types of salalen titanium(IV) complexes (Scheme 1) and successfully applied them to produce ultrahigh-molecular-weight ethylene.[40]

The fluorinated salalen titanium(IV) complex (F-salalen)$TiCl_2$ performed relatively high catalytic activity and thermal stability on ethylene homopolymerization due to the electron withdrawing conjugated effect, as well as exhibited quasi-living characteristic. Recently, we found that both (H-salalen)$TiCl_2$ and (F-salalen)$TiCl_2$ were able to catalyze copolymerization of ethylene with long chain α-olefin like 1-octene and 1-decene. In particular, ultrahigh-molecular-weight poly(ethylene-*co*-1-octene) can be obtained by (F-salalen)$TiCl_2$/MAO under certain reaction conditions, which is an exciting result and worthy of further study.

Results and discussion

This work was focused on the copolymerization of ethylene with 1-octene including catalytic behaviour as well as the analysis and characterization of the resultant copolymers. Two salalen titanium complexes were synthesized as comparison according to our previous work. Copolymerization of ethylene with 1-octene were carried out at different temperatures using (H-salalen)$TiCl_2$ and (F-salalen)$TiCl_2$ activated by MAO, and the results were summarized in Table 1.

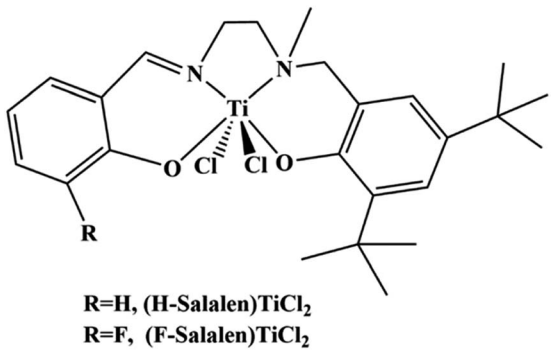

Scheme 1 Structure of (H-salalen)$TiCl_2$ and (F-salalen)$TiCl_2$.

As displayed in Table 1, both salalen type titanium complexes ((F-salalen)$TiCl_2$ and (H-salalen)$TiCl_2$) could catalyze the copolymerization of ethylene with 1-octene under MAO activation to produce poly(ethylene-*co*-1-octene) with high molecular weight. Note that (F-salalen)$TiCl_2$/MAO showed higher catalytic activity, which was more than twofold that of (H-salalen)$TiCl_2$ at 50 °C. In particular, as depicted by Fig. 1, (F-salalen)$TiCl_2$/MAO were able to afforded poly(ethylene-*co*-1-octene) with ultrahigh molecular weight of 1.89×10^6 and 1.23×10^6 g mol^{-1} respectively when polymerization temperature at 30 and 40 °C. In contrast, (H-salalen)$TiCl_2$ can only provide copolymers with molecular weight lower than 7.1×10^5 g mol^{-1} under the same polymerization conditions. Moreover, the copolymers obtained by (F-salalen)$TiCl_2$/MAO exhibited narrower molecular weight distribution ($M_w/M_n \sim 2.6$) and higher 1-octene incorporation than (H-salalen)$TiCl_2$/MAO. These results were in agreement with those obtained from the ethylene homopolymerization based on the electronically flexible property and electron withdrawing conjugated effect consisting of fluorine (F), phenyl ring, imine and titanium(IV) species.[41–44] Therefore, there was a reason to believe that the (F-salalen)$TiCl_2$/MAO catalyst revealed stronger thermal stability and better catalytic performance for coordination copolymerization of ethylene with 1-octene than (H-salalen)$TiCl_2$ catalyst.

In order to further investigate the catalytic behaviour of (F-salalen)$TiCl_2$/MAO for the copolymerization of ethylene with 1-octene under different polymerization conditions, the representative polymerization results at various temperatures, Al/Ti molar ratios and monomer feed ratios were listed in Table 2. The catalytic activity of copolymerization of ethylene with 1-octene was higher than ethylene homopolymerization because of the "comonomer effect". The introduction of 1-octene into polyethylene chain reduced the crystallinity and improved the solubility of polymer, leading to easier exposure and diffusion of active centers. However, the molecular weight of copolymerization products had drop sharply from 2.64×10^6 to 0.87×10^6 g mol^{-1}, and the products were hardly observed in the 1-octene homopolymerization. This probably due to long-chain 1-octene with large steric hindrance were more difficult to coordinate with active species and insert into the polyethylene chain.

To explore the effect of polymerization temperature on copolymers produced by (F-salalen)$TiCl_2$/MAO, different polymerization temperatures involving 30, 40, 50, 70, 90 °C were set (entry 3–7, Table 2) when 1-octene concentration was 1.0 mol L^{-1}. Catalytic activity increased steadily from 35.6×10^3 g polymer (mol Ti)$^{-1}$ h^{-1} at 30 °C to 141.0×10^3 g polymer (mol Ti)$^{-1}$ h^{-1} at 70 °C and still maintained a moderate high level at 90 °C, implying good thermal stability of (F-salalen)$TiCl_2$. The increase of activity at 30–70 °C came from the increase of the number of active species and the thermal

Table 1 The results of copolymerization of ethylene with 1-octene using (H-salalen)$TiCl_2$ and (F-salalen)$TiCl_2$ in the presence of MAO[a]

Entry	Complex	T_p (°C)	Activity[b]	M_w[c] $\times 10^{-6}$	M_w/M_n[c]	T_m[d] (°C)	ΔH[d] (J g^{-1})	X_c[d] (%)	1-Oct. cont.[e] (mol%)
1	(H-Salalen)$TiCl_2$	30	10.2	0.71	2.7	127.0	183.4	62.6	0.3
2		40	34.7	0.49	3.2	123.7	114.7	39.1	1.3
3		50	39.9	0.05	3.6	122.9	105.0	35.8	2.0
4	(F-Salalen)$TiCl_2$	30	35.6	1.89	2.1	125.0	177.3	60.5	0.9
5		40	42.0	1.23	2.2	124.1	141.0	48.1	1.8
6		50	92.3	0.87	2.6	119.4	80.6	27.5	3.1

[a] Polymerization conditions: catalyst, 20.0 μmol; Al/Ti = 600; 1-octene, 1.0 mol L^{-1}; ethylene pressure, 15 atm; total volume, 70 mL; reaction time, 30 min. [b] In 10^3 g polymer (mol Ti)$^{-1}$ h^{-1}. [c] g mol^{-1}, determined by HT-GPC in 1,2,4-TCB *versus* polystyrene standard. [d] Determined by DSC at a heating rate of 10 °C min^{-1} and used the second heating curves. [e] 1-Octene incorporation (mol%) estimated by ^{13}C NMR spectra.

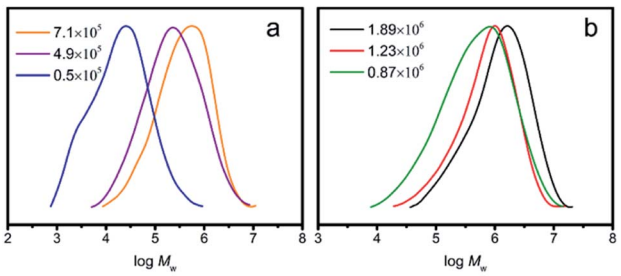

Fig. 1 (a) GPC profile of poly(ethylene-*co*-1-octene) formed using (H-salalen)$TiCl_2$/MAO at 30, 40, and 50 °C; (b) GPC profile of poly(-ethylene-*co*-1-octene) formed using (F-salalen)$TiCl_2$/MAO at 30, 40, and 50 °C.

stability was probably due to the electron withdrawing conjugate effect consisting of F, phenyl ring, imine and titanium(IV). Besides, the increase in the number of active species reduced the number-average chain length and thus the molecular weight of copolymers declined. At 30–50 °C, ethylene/1-octene copolymers with ultrahigh-molecular-weight could be prepared in 30 min. While the molecular weight was less than 1.0×10^6 g mol^{-1} at higher polymerization temperatures, and it decreased to 1.0×10^5 g mol^{-1} at 90 °C. Besides, molecular weight distribution became broader when temperature increased because the chain transfer rate increased rapidly or appeared other active centers at high temperature.[45,46] Appropriate heating may help the insertion of 1-octene according to entries 3–5 in Table 2, but when the temperature rose to 70 °C the content of 1-octene in copolymers started to decline instead.

Influence of Al/Ti molar ratios on the copolymerization of ethylene with 1-octene using (F-salalen)$TiCl_2$/MAO was then investigated. Table 2 showed that the catalytic activity increased with the increase of Al/Ti molar ratios from 200 to 600. On the one hand, less MAO was not enough to remove impurities unfavorable to the catalyst like moisture and oxygen in the polymerization system. On the other hand, only a sufficient amount of cocatalyst could fully activate the catalyst, as MAO could capture the chlorine atoms from the (F-salalen)$TiCl_2$ complex and formed alkyl ligand and vacancy in the central metal to form the active species to promote copolymerization. However, the activity suddenly dropped sharply when the Al/Ti mole ratio reached 800 (Table 2, entry 10). This is probably due to excessive MAO reduced the titanium metal with high

Table 2 The results of copolymerization of ethylene with 1-octene using (F-salalen)$TiCl_2$ in the presence of MAO[a]

Entry	Al/Ti (mol mol^{-1})	T_p (°C)	1-Oct. feed (mol L^{-1})	Activity[b]	M_w[c] $\times 10^{-6}$	M_w/M_n[c]	T_m[d] (°C)	ΔH[d] (J g^{-1})	X_c[d] (%)	1-Oct. cont.[e] (mol%)
1	600	50	0	56.5	2.64	2.4	134.6	204.5	69.8	0
2[f]	600	50	1.2	n.d	—	—	—			—
3	600	30	1.0	35.6	1.89	2.1	125.0	177.3	60.5	0.9
4	600	40	1.0	42.0	1.23	2.2	124.1	141.0	48.1	1.8
5	600	50	1.0	92.3	0.87	2.6	119.4	80.6	27.5	3.1
6	600	70	1.0	141.0	0.22	3.2	120.5	85.3	29.1	2.0
7	600	90	1.0	101.2	0.10	3.9	120.9	136.9	46.7	1.9
8	200	50	1.0	63.5	1.64	1.9	123.5	101.1	34.5	2.0
9	400	50	1.0	87.0	1.24	2.1	123.3	83.8	28.6	2.6
10	800	50	1.0	35.0	0.57	3.4	123.5	101.4	34.6	2.2
11	600	50	0.2	79.8	1.26	2.7	128.7	172.1	58.7	1.2
12	600	50	0.4	127.5	1.00	2.9	124.4	160.6	54.8	1.7
13	600	50	0.8	132.5	0.89	2.6	122.3	92.2	31.5	2.8
14	600	50	2.0	64.0	0.78	2.7	117.9	65.8	22.5	6.4

[a] Polymerization conditions: catalyst, 20.0 μmol; ethylene pressure, 15 atm; total volume, 70 mL; reaction time, 30 min. [b] 10^3 g polymer (mol Ti)$^{-1}$ h^{-1}. [c] g mol^{-1}, determined by HT-GPC in 1,2,4-TCB *versus* polystyrene standard. [d] Determined by DSC at a heating rate of 10 °C min^{-1} and used the second heating curves. [e] 1-Octene incorporation (mol%) estimated by ^{13}C NMR spectra. [f] 1-Octene homopolymerization, ethylene pressure, 0 atm.

oxidation state to low oxidation state, resulting in a decrease in the number of effective active species.[47] In addition, lower Al/Ti mol ratio resulted in the formation of higher molecular weight copolymer, for example, the copolymer with ultrahigh molecular weight of 1.64×10^6 g mol^{-1} and narrow molecular weight distribution ($M_w/M_n = 1.9$) could be obtained at Al/Ti = 200 (Table 2, entry 8). Correspondingly, the molecular weight started to decrease as well as molecular weight distribution became broader with the increase of Al/Ti molar ratios, which is due to the gradually intensive chain transfer reaction to MAO.

It was obvious from Table 2 that the copolymerization yield, the molecular weight, and the 1-octene incorporation of the copolymers related to the 1-octene concentration in the feed (entry 1, 5, 11–14). When the concentration of 1-octene increased from 0 mol L^{-1} to 1.0 mol L^{-1}, the catalytic activity continued to increase. But after 1-octene concentration reached a higher value of 2.0 mol L^{-1}, the copolymer yield started to drop again. Molecular weight of copolymers kept decreasing accompanied by the increase of 1-octene concentration. These variations on catalytic activity and molecular weight brought by the introduction of 1-octene were coincided with "comonomer effect" in Ziegler–Natta catalytic system and metallocene catalysts.[48] Furthermore, the content of 1-octene in the copolymer increased gradually and reached 6.4% at 2.0 mol L^{-1}.

The ^{13}C NMR spectrum in Fig. 2 showed that the resonance at 30.0 ppm arose from polyethylene sequences was the most abundant peak, which could be assigned to CH_2 in polyethylene chain. However, those signals dated from continuous 1-octene block sequence (OOO) or alternating sequence (EOEO) were hardly observed, and the ethylene average sequence length was calculated as 13.8 through ^{13}C NMR triad distribution (Table S2†), suggesting that 1-octene units were isolated by long ethylene segments.

The differential scanning calorimeter (DSC) was used to determine the melting temperature of copolymers with different 1-octene incorporation, and the second heating curves were displayed in Fig. 3. Compared with ultrahigh molecular weight polyethylene produced by (F-salalen)$TiCl_2$/MAO, copolymers with introduction of 1-octene exhibited decline in melting temperature. With the increase of 1-octene content in poly(ethylene-*co*-1-octene), the melting temperatures also showed decrease. When the 1-octene content reached the maximum value of 6.4% at 2.0 mol L^{-1}, the melting temperature was as low as 117.9 °C. These copolymers showed higher melting temperature than many other previously reported poly(ethylene-*co*-1-octene) with similar comonomer incorporation because of the longer polyethylene segments.[49,50] It is worth noting that some shoulders can be seen at lower temperatures for samples with higher 1-octene incorporation (*e.g.* entry 13). We suggest that the main chain was divided into polyethylene segments with different length due to the heterogeneous distribution of 1-octene. Consequently, the shoulder peaks might originate from the crystallization of some shorter polyethylene segments. This heterogeneous distribution can be proved by DSC-SSA thermogram (Fig. S2†). There were nine narrow peaks appeared at 60–100 °C in the SSA thermogram of entry 13, denoting about nine polyethylene segments with different length, which caused the wide shoulder in DSC heating curve.

The crystallinity of these copolymers produced by (F-salalen)$TiCl_2$/MAO were also studied. The X-ray diffraction patterns of the resultant ultrahigh-molecular-weight polyethylene and ethylene/1-octene copolymers with different 1-octene content were shown in Fig. 4. It could be seen that there were two obvious peaks at the 2θ values of 21.6° and 24.0° corresponded to 110 and 200 crystal planes of polyethylene orthorhombic crystal form, respectively.[50] The crystallinity of copolymers declined from 72.7% to 23.4% (Table S3†) with the increase of 1-octene concentration in the feed, exhibiting a trend consisted with crystallinity results calculated by DSC. The low incorporation of 1-octene (≤6.4%) also means that only a little 1-octene units into polyethylene chain can affect the crystallization of the copolymer significantly. Moreover, a broad peak at 19–20° in the copolymer diffraction pattern appeared and gradually became obvious as the content of 1-

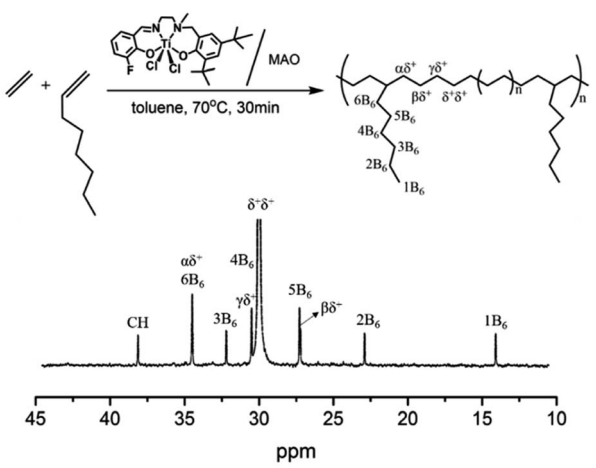

Fig. 2 ^{13}C NMR spectrum of poly(ethylene-*co*-1-octene) obtained using the (F-salalen)$TiCl_2$/MAO (entry 6 in Table 2).

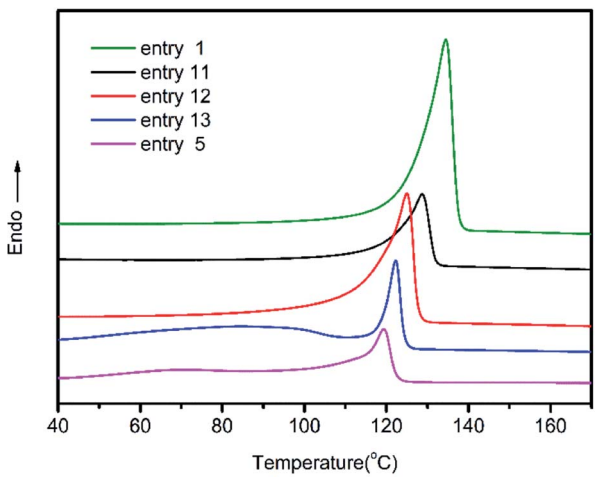

Fig. 3 DSC profiles of poly(ethylene-*co*-1-octene) with different 1-octene incorporation obtained from entry 1, 5, 11–13 in Table 2.

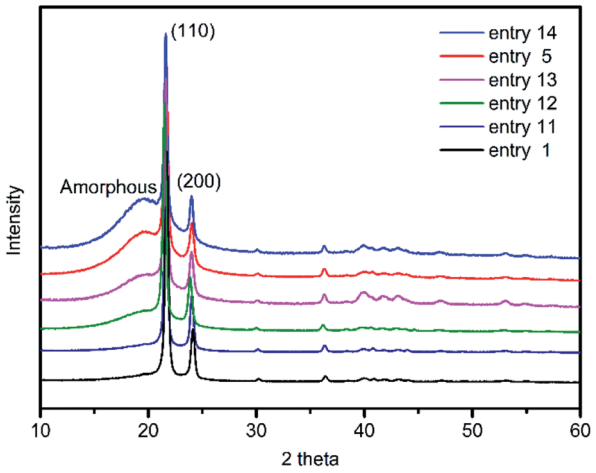

Fig. 4 X-ray diffractograms of poly(ethylene-*co*-1-octene) with different 1-octene incorporation in Table 2, from top to bottom: entry 14, entry 5, entry 13, entry 12, entry 11, entry 1.

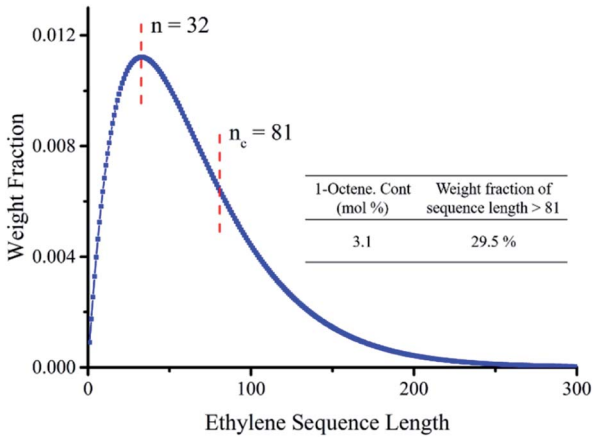

Fig. 5 Ethylene sequence length distribution of ethylene/1-octene (entry 14 in Table 2).

octene increases, denoting that the amorphous part of the copolymer was gradually increasing.

In order to further explore the distribution of ethylene and 1-octene in the copolymer chains, the reactivity ratios were calculated by the triad distribution from the ^{13}C NMR spectrum (Table S2†) and provided the values $r_E = 11.25$, $r_O = 0.15$ and $r_E r_O = 1.69$. The calculation results showed the preference for ethylene incorporation promoted the formation of long polyethylene sequences along the copolymer chain, suggesting that (F-salalen)$TiCl_2$/MAO tends to produce random ethylene/1-octene copolymer.

The melting temperature and crystalline of ethylene/1-octene copolymer are always related to the ethylene sequence length distribution. Using the value of reactivity ratios, the ethylene sequence distribution can be calculated by Flory's theory:[51]

$$W_n = n(1-p)^2 p^{n-1} \quad (1)$$

where W_n is the normalized weight fraction of the sequence of n ethylene units. p is the sequence propagation probability and calculated through the expression:

$$p = 1 - \frac{1 - [1 - 4(1 - r_E r_O)X_E(1 - X_E)]^{1/2}}{2(1 - r_E r_O)X_E} \quad (2)$$

The ethylene mole fraction X_E of sample entry 6 in Table 1 and $r_E r_O = 1.69$ were used in the expression (2). Finally the ethylene sequence distribution of ethylene/1-octene copolymer obtained by (F-salalen)$TiCl_2$/MAO was shown in Fig. 5. The most probable ethylene unit n appeared at 32. To explore the relationship between DSC curve and ethylene sequence length, the following expression (3) and (4) were used:[52]

$$\frac{1}{T_m^c} = \frac{1}{T_m^0} - \frac{R}{\Delta H_u} \ln p \quad (3)$$

$$T_m^f = T_m^c\left(1 - \frac{2\sigma_e \alpha_0}{\Delta H_u n_c}\right) \quad (4)$$

where T_m^c, T_m^f are the equilibrium melting temperature of the copolymer and the DSC final melting temperature respectively. Other parameters T_m^0 is the melting temperature of polyethylene perfect crystal (418.7 K), ΔH_u is the heat of fusion for a repeat unit (8.284 kJ mol^{-1}), σ_e is the surface energy of polyethylene (90 mJ m^{-2}), and α_0 is cross-sectional area of a chain (1.10×10^5 m^2 mol^{-1}). Substituted final melting temperature of sample entry 6 in Table 1 (401.15 K) into the above formulas, the corresponding crystal sequence length n_c was calculated as 81. It can be seen from Fig. 5 that n_c was much bigger than the most probable ethylene unit ($n = 32$). The weight fraction of ethylene sequence length > 81 units was 29.5%, the result was closed to crystallinity calculated with DSC (27.5%) and XRD (28.4%), indicating that the melting temperature and crystallization of copolymer were highly correlated with ethylene sequence length distribution.[53] Moreover, there were some reports pointed out that the melting temperature of copolymers depended more on the sequence randomness instead of the most probable ethylene unit.[52]

Experimental

Materials

All operations involving anhydrous and anoxic should be performed using standard Schlenk line techniques or in a glove box filled with high purity nitrogen. Ethylene (99.9%, GQ-gas) and nitrogen (99.999%, GQ-gas) were used directly without any pretreatment. Toluene (Analytical Reagent, Guangzhou Brand) was refluxed in the presence of sodium or potassium for at least 10 h, using benzophenone as indicator until the mixture turned blue. 1-Octene (98%, Aladdin) was added calcium hydride and stirred overnight and then distilled for use. Methylaluminoxane (MAO) was purchased from AkzoNobel as 10 wt% Al toluene solution. The salalen titanium(IV) complexes used in this work was synthesized as described in the literature,[40] and it's structure can be seen in Scheme 1.

Copolymerization of ethylene with 1-octene

Copolymerization of ethylene with 1-octene was carried out in a 250 mL autoclave equipped with program temperature controller and mechanical stirring. The autoclave was firstly heated to 150 °C for 3 hours under vacuum in order to remove moisture and oxygen, and then cooled to the reaction temperature. Toluene, 1-octene, and methylaluminoxane (MAO) solution were sequentially injected into the autoclave and stirred for 5 min. The copolymerization was started by charging the salalen titanium(IV) complexes (pre-dissolved in toluene) into the autoclave and then rose the ethylene pressure to 15 atm. The polymerization temperature was kept by the program temperature controller, and the error did not exceed ±2 °C. After the polymerization reached 30 min at the reaction temperature, stopped ethylene feed and injected 5 mL methanol into the autoclave to terminated polymerization. The resulting mixture was poured into acidic ethanol (20 : 1 ethanol/HCl) and stirred for 12 hours. The copolymers were finally collected after washing with ethanol, filtration and dried under vacuum at 50 °C to a constant weight.

Polymer characterization

Molecular weight (M_w) and molecular weight distribution (M_w/M_n) were measured by using high-temperature chromatograph (GPC) on a PL-GPC 220 type at 150 °C. The instrument was equipped with a refractive index detector and used 1,2,4-trichlorobenzene at a flow rate of 1.0 mL min^{-1} as the mobile phase, samples were dissolved in 1,2,4-trichlorobenzene as 1 mg mL^{-1} solution. The calibration curves were made by monodisperse polystyrene with a sample solution concentration of 0.5–1.0 mg mL^{-1}. ^{13}C NMR spectra of the copolymers were obtained with a Bruker Avance III 500 MHz NMR instrument at 120 °C. The samples were dissolved as 100 mg mL^{-1} in the 10 mm high temperature NMR tubes, using a mixed solvent of deuterated *o*-dichlorobenzene/*o*-dichlorobenzene with a volume ratio of 1 : 1. The 1-octene contents, ethylene average sequence length and triad sequential distribution of the copolymers were calculated from the ^{13}C NMR spectra. The thermal properties of polymers were determined by differential scanning calorimetry (DSC) on a DSC-4000 from PerkinElmer company under N_2 atmosphere. The follow programs were set: firstly weighed 3–5 mg polymers and heated it to 180 °C with a rate of 10 °C min^{-1}, kept at 180 °C for 5 min to remove the thermal history. Then cooled down to 30 °C with a rate of 10 °C min^{-1}, kept at 30 °C for 5 min followed by heating to 180 °C with a rate of 10 °C min^{-1} again, finally recorded the second heating curve. The crystal structure of samples was determined by X-ray diffraction (XRD) on a RIGAKU D-MAX 2200 at room temperature. Using Cu Kα radiation and the diffraction scans from 10°–80° with a rate of 10° min^{-1}.

Conclusions

Two salalen titanium complexes, (H-salalen)$TiCl_2$ and (F-salalen)$TiCl_2$ are firstly used to catalyze the copolymerization of ethylene with 1-octene in the presence of methylaluminoxane (MAO) with moderate activity, in which (F-salalen)$TiCl_2$ shows better catalytic performance and higher thermal stability owing to the electron withdrawing conjugated effect introduced by F atom. Under the optimized polymerization conditions, (F-salalen)$TiCl_2$/MAO can produce ultrahigh-molecular-weight poly(ethylene-*co*-1-octene) with relatively narrow molecular weight distribution. The 1-octene content of these resultant copolymers was controlled from 0.9 to 6.4 mol% through adjusting the 1-octene feed concentration from 0.2 to 2.0 mol L^{-1}. Based on DSC and XRD characterization, high molecular weight and higher crystallinity lead to relatively high melting temperature (128.7–117.9 °C) of the copolymers, and the results are agreed well with ethylene sequence length distribution. The molecular chain structure of the copolymers is characterized by ^{13}C NMR, suggesting that long ethylene sequences in poly(ethylene-*co*-1-octene) chains are segregated by isolated 1-octene units. The reactivity ratios ($r_E = 11.25$, $r_O = 0.15$, $r_E r_O = 1.69$) calculated by the triad sequential distribution indicates that (F-salalen)$TiCl_2$/MAO tends to produce random ethylene/1-octene copolymers.

Conflicts of interest

There are no conflicts to declare.

Acknowledgements

This work was supported by the National Natural Science Foundation of China (51773228, 51573212).

Notes and references

1 M. Ronellenfitsch, T. Gehrmann, H. Wadepohl and M. Enders, *Macromolecules*, 2016, **50**, 35–43.
2 J. Xia, Y. Zhang, S. Kou and Z. Jian, *J. Catal.*, 2020, **390**, 30–36.
3 L. Guo, K. Lian, W. Kong, S. Xu, G. Jiang and S. Dai, *Organometallics*, 2018, **37**, 2442–2449.
4 D. Romano, N. Tops, E. Andablo-Reyes, S. Ronca and S. Rastogi, *Macromolecules*, 2014, **47**, 4750–4760.
5 A. Pandey, Y. Champouret and S. Rastogi, *Macromolecules*, 2011, **44**, 4952–4960.
6 Z. Zhou, C. Anklin, R. Cong, X. Qiu and R. Kuemmerle, *Macromolecules*, 2021, **54**, 757–762.
7 X. Hu, C. Geng, G. Yang, Q. Fu and H. Bai, *RSC Adv.*, 2015, **5**, 54488–54496.
8 S. Ohta, Y. Kasai, T. Toda, K. Nishii and M. Okazaki, *Polym. J.*, 2018, **51**, 345–349.
9 M. Białek and K. J. P. Czaja, *Polymer*, 2000, **41**, 7899–7904.
10 Z. Zhao, T. Mikenas, V. A. Zakharov, M. Nikolaeva, M. Matsko, E. Bessudnova and W. J. P. J. Wu, *Polyolefins J.*, 2019, **6**, 117–126.
11 G. Zanchin, F. Bertini, L. Vendier, G. Ricci, C. Lorber and G. Leone, *Polym. Chem.*, 2019, **10**, 6200–6216.
12 W. Liu, A. T. Ojo, W.-J. Wang, H. Fan, B.-G. Li and S. Zhu, *Polym. Chem.*, 2015, **6**, 3800–3806.
13 X. Ren, F. Guo, H. Fu, Y. Song, Y. Li and Z. Hou, *Polym. Chem.*, 2018, **9**, 1223–1233.

14 S. M. M. Mortazavi, H. Arabi, G. Zohuri, S. Ahmadjo, M. Nekoomanesh and M. Ahmadi, *Polym. Int.*, 2010, **59**, 1258–1265.
15 E. S. Cueny and C. R. Landis, *ACS Catal.*, 2019, **9**, 3338–3348.
16 K. Kunz, G. Erker, S. Döring, R. Fröhlich and G. Kehr, *J. Am. Chem. Soc.*, 2001, **123**, 6181–6182.
17 U. G. Joung, C. J. Wu, S. H. Lee, C. H. Lee, E. J. Lee, W.-S. Han, S. O. Kang and B. Y. J. O. Lee, *Organometallics*, 2006, **25**, 5122–5130.
18 J. H. Park, S. H. Do, A. Cyriac, H. Yun and B. Y. Lee, *Dalton Trans.*, 2010, **39**, 9994–10002.
19 P. S. Chum and K. W. Swogger, *Prog. Polym. Sci.*, 2008, **33**, 797–819.
20 K. Soga, T. Uozumi, S. Nakamura, T. Toneri, T. Teranishi, T. Sano, T. Arai and T. Shiono, *Macromol. Chem. Phys.*, 1996, **197**, 4237–4251.
21 S.-W. Zhang, L.-P. Lu, Y.-Y. Long and Y.-S. Li, *J. Polym. Sci., Part A: Polym. Chem.*, 2013, **51**, 5298–5306.
22 W. Liu, K. Zhang, H. Fan, W.-J. Wang, B.-G. Li and S. Zhu, *J. Polym. Sci., Part A: Polym. Chem.*, 2013, **51**, 405–414.
23 S. Saadat, J. B. P. Soares, P. J. DesLauriers and J. S. Fodor, *Macromol. React. Eng.*, 2020, **14**(2), 1900032.
24 S. Guo, H. Fan, Z. Bu, B. G. Li and S. Zhu, *Macromol. Rapid Commun.*, 2015, **36**, 286–291.
25 T. J. Williams, J. V. Lamb, J.-C. Buffet, T. Khamnaen and D. O'Hare, *RSC Adv.*, 2021, **11**, 5644–5650.
26 K. Matsumoto, B. Saito and T. Katsuki, *Chem. Commun.*, 2007, 3619–3627, DOI: **10.1039/b701431g**.
27 A. Yeori, S. Gendler, S. Groysman, I. Goldberg and M. Kol, *Inorg. Chem. Commun.*, 2004, **7**, 280–282.
28 A. Cohen, G. W. Coates and M. Kol, *J. Polym. Sci., Part A: Polym. Chem.*, 2013, **51**, 593–600.
29 K. Press, A. Cohen, I. Goldberg, V. Venditto, M. Mazzeo and M. Kol, *Angew. Chem., Int. Ed. Engl.*, 2011, **50**, 3529–3532.
30 K. Huang, S. Zhou, D. Zhang, X. Gao, Q. Wang and Y. Lin, *J. Organomet. Chem.*, 2013, **741–742**, 83–90.
31 A. Berkessel, T. Günther, Q. Wang and J.-M. Neudörfl, *Angew. Chem.*, 2013, **125**, 8625–8629.
32 Y. Sawada, K. Matsumoto and T. Katsuki, *Angew. Chem., Int. Ed. Engl.*, 2007, **46**, 4559–4561.
33 E. P. Talsi, A. A. Bryliakova and K. P. Bryliakov, *Chem. Rec.*, 2016, **16**, 924–939.
34 X. Ji, W. Yao, X. Luo, W. Gao and Y. Mu, *New J. Chem.*, 2016, **40**, 2071–2078.
35 Y.-L. Duan, Z.-J. Hu, B.-Q. Yang, F.-F. Ding, W. Wang, Y. Huang and Y. Yang, *Dalton Trans.*, 2017, **46**, 11259–11270.
36 K. Nie, W. Gu, Y. Yao, Y. Zhang and Q. Shen, *Organometallics*, 2013, **32**, 2608–2617.
37 A. Pilone, N. De Maio, K. Press, V. Venditto, D. Pappalardo, M. Mazzeo, C. Pellecchia, M. Kol and M. Lamberti, *Dalton Trans.*, 2015, **44**, 2157–2165.
38 X. Zhang, Y. Liu, Y. Chen, Z. Zhang, D. Fan and L. Xingqiang, *Inorg. Chem. Commun.*, 2014, **48**, 69–72.
39 H. Engler, M. Lansing, C. P. Gordon, J.-M. Neudörfl, M. Schäfer, N. E. Schlörer, C. Copéret and A. Berkessel, *ACS Catal.*, 2021, **11**, 3206–3217.
40 S. Li, Y. Zhu, H. Liang, X. Xie, Y. Zhan, G. Liang and F. Zhu, *RSC Adv.*, 2019, **9**, 41824–41831.
41 G. Xie and C. Qian, *J. Polym. Sci., Part A: Polym. Chem.*, 2008, **46**, 211–217.
42 M. A. M. Capozzi, F. Capitelli, A. Bottoni, M. Calvaresi and C. Cardellicchio, *ChemCatChem*, 2013, **5**, 210–219.
43 G. Xie and C. Qian, *J. Polym. Sci., Part A: Polym. Chem.*, 2008, **46**, 211–217.
44 T. Li, W. Song, H. Ai, Q. You, A. Zhang and G. Xie, *J. Polym. Res.*, 2014, **22**, 631.
45 M. Khoshsefat, S. Ahmadjo, S. Mortazavi, G. Zohuri and J. Soares, *New J. Chem.*, 2018, **42**, 8334–8337.
46 M. Khoshsefat, A. Dechal, S. Ahmadjo, S. M. M. Mortazavi, G. Zohuri and J. B. Soares, *Eur. Polym. J.*, 2019, **119**, 229–238.
47 L. Zhu, H. Yu, L. Wang and Y. Xing, *Mater. Today Commun.*, 2021, **29**, 102801.
48 M. Yin, Z. Zhang, Y. Xiong, M. Liu, Y. Zhang and P. Mi, *Chem. Res. Chin. Univ.*, 2019, **35**, 1089–1094.
49 E. Szuromi, J. Klosin and K. A. Abboud, *Organometallics*, 2011, **30**, 4589–4597.
50 M. Wannaborworn, P. Praserthdam and B. Jongsomjit, *Molecules*, 2011, **16**, 373–383.
51 M. Atiqullah, S. Adamu and A.-H. M. Emwas, *J. Taiwan Inst. Chem. Eng.*, 2017, **76**, 141–155.
52 S. Hosoda, Y. Nozue, Y. Kawashima, K. Suita, S. Seno, T. Nagamatsu, K. B. Wagener, B. Inci, F. Zuluaga and G. Rojas, *Macromolecules*, 2011, **44**, 313–319.
53 S. Guo, H. Fan, Z. Bu, B.-G. Li and S. Zhu, *Polymer*, 2015, **80**, 109–114.